

Atomic ionization of germanium due to neutrino magnetic moments

Jiunn-Wei Chen,^{1,2} Hsin-Chang Chi,³ Keh-Ning Huang,^{4,5,1} C.-P. Liu,³ Hao-Tse Shiao,¹ Lakhwinder Singh,^{6,7} Henry T. Wong,⁶ Chih-Liang Wu,¹ and Chih-Pan Wu¹

¹Department of Physics, National Taiwan University, Taipei 10617, Taiwan

²National Center for Theoretical Sciences and Leung Center for Cosmology and Particle Astrophysics, National Taiwan University, Taipei 10617, Taiwan

³Department of Physics, National Dong Hwa University, Shoufeng, Hualien 97401, Taiwan

⁴Department of Physics, Sichuan University, Chengdu, Sichuan, China

⁵Department of Physics, Fuzhou University, Fuzhou, Fujian, China

⁶Institute of Physics, Academia Sinica, Taipei 11529, Taiwan

⁷Department of Physics, Banaras Hindu University, Varanasi 221005, India

An *ab initio* calculation of atomic ionization of germanium (Ge) by neutrinos was carried out in the framework of multiconfiguration relativistic random phase approximation. The main goal is to provide a more accurate cross section formula than the conventional one, which is based on the free electron approximation, for searches of neutrino magnetic moments with Ge detectors whose threshold is reaching down to the sub-keV regime. Limits derived with both methods are compared, using reactor neutrino data taken with low threshold germanium detectors.

Neutrino magnetic moments (NMM) describe possible electromagnetic couplings of the neutrino with the photon via its spin (for reviews, see e.g., Refs. [1, 2]). In the minimally-extended Standard Model (SM), massive neutrinos acquire non-vanishing, but extremely small, NMMs through electroweak radiative corrections: $\mu_\nu \simeq 3 \times 10^{-19} \mu_B [m_\nu/1 \text{ eV}]$ in units of the the Bohr magneton μ_B [3–5]. The current upper limits set on μ_ν are orders of magnitude larger than this SM prediction. A large NMM, if observed, will not only imply sources of new physics, but also have significant impact to the evolution of early Universe and stellar nucleosynthesis (see e.g., Ref. [6]). Furthermore, it might favor Majorana neutrinos [7].

The current experimental limits on μ_ν are extracted from the energy spectra of recoil electron in neutrino scattering off detectors. The scattering cross section contains two incoherent contributions: one from the weak interaction, σ_w , which preserves the neutrino helicity, and the other from the magnetic interaction, σ_μ , which flips it. When the incident neutrino energy (E_ν) and the energy loss to the detector (T) are high enough so that the binding effects of electrons can be ignored, the neutrino-free-electron scattering formula is [8]

$$\frac{d\sigma_w^{(0)}}{dT} = \frac{G_F^2 m_e}{2\pi} \left[g_\nu^2 + g_\nu'^2 \left(1 - \frac{T}{E_\nu} \right)^2 - g_\nu g_\nu' \frac{m_e T}{E_\nu^2} \right], \quad (1)$$

$$\frac{d\sigma_\mu^{(0)}}{dT} = 4\pi\alpha\mu_\nu^2 \left(\frac{1}{T} - \frac{1}{E_\nu} \right), \quad (2)$$

where G_F and α are the Fermi and fine structure constants; the flavor dependent weak couplings, depending on the Weinberg angle θ_W , are $g_{\nu_e} = 1 + 2\sin^2\theta_W$, $g_{\nu_{\mu,\tau}} = -1 + 2\sin^2\theta_W$, $g_{\nu_e,\mu,\tau}' = 2\sin^2\theta_W$, and interchange $g_{\bar{\nu}(\nu)} \leftrightarrow g_{\nu(\bar{\nu})}'$ for corresponding antineutrinos. Based on this formula, several groups recently published their results: $\mu_{\bar{\nu}_e} < 2.9 \times 10^{-11} \mu_B$ [9] (GEMMA) and

$\mu_{\bar{\nu}_e} < 7.4 \times 10^{-11} \mu_B$ [10] (TEXONO) for reactor antineutrinos, and $\mu_{\nu_\odot} < 5.4 \times 10^{-11} \mu_B$ [11] (Borexino) for solar neutrinos.

One way to improve the experimental sensitivities is to lower the detector threshold so that events with low T can be registered. Comparing Eqs. (1,2), one sees that for $T \ll E_\nu$, the weak part remains constant while the magnetic part increases as $1/T$, which indicates an enhanced sensitivity to μ_ν . The GEMMA and TEXONO experiments both used germanium (Ge) semiconductor detectors, with thresholds at $T = 2.8$ and 12 keV , respectively, for the reported bounds on $\mu_{\bar{\nu}_e}$ quoted above. Recently, the threshold of Ge detectors has been further lowered down to the sub-keV regime for light WIMP searches and for the studies of neutrino-nucleus coherent scattering [12–14].

As the kinematics in neutrino scattering with sub-keV energy transfer starts to overlap with atomic scales, how the atomic binding effects modify the above free scattering formula becomes an essential issue. This problem has recently been intensively re-visited because of a derivation that atomic structure can greatly enhance the magnetic cross section by orders of magnitude over the free scattering formula at low T [15], in contrast to previous studies all showing suppression [16–20]. While latter works [21–24] justified, with generic arguments and schematic calculations, that atomic binding effects suppress the scattering cross sections and the usability of a simple free electron approximation [17], it remains challenging to obtain a differential cross section formula at low T with a reasonable error estimate. In this letter, we address the case of germanium and report an *ab initio* calculation of germanium ionization by scattering of reactor antineutrinos

$$\bar{\nu}_e + \text{Ge} \rightarrow \bar{\nu}_e + \text{Ge}^+ + e^-.$$

Taking an ultrarelativistic limit for neutrinos $m_\nu \rightarrow 0$, the double differential cross sections for unpolarized scattering with complex atomic targets are expressed as

$$\begin{aligned} & \frac{d\sigma_w}{dTd\Omega} \\ &= \frac{G_F^2}{2\pi^2} (E_\nu - T)^2 \cos^2 \frac{\theta}{2} \left[R_{00}^{(w)} - \frac{T}{q} R_{03+30}^{(w)} + \frac{T^2}{q^2} R_{33}^{(w)} \right. \\ & \quad \left. + \left(\tan^2 \frac{\theta}{2} + \frac{Q^2}{2q^2} \right) R_{11+22}^{(w)} + \tan \frac{\theta}{2} \sqrt{\tan^2 \frac{\theta}{2} + \frac{Q^2}{q^2}} R_{12+21}^{(w)} \right], \end{aligned} \quad (3)$$

$$\begin{aligned} & \frac{d\sigma_\mu}{dTd\Omega} \\ &= \alpha \mu_\nu^2 \left(1 - \frac{T}{E_\nu} \right) \left[\frac{(2E_\nu - T)^2 Q^2}{q^4} R_{00}^{(\gamma)} \right. \\ & \quad \left. + \frac{4E_\nu(E_\nu - T) - Q^2}{2q^2} R_{11+22}^{(\gamma)} \right], \end{aligned} \quad (4)$$

where θ is the neutrino scattering angle, $q = |\vec{q}|$ is the magnitude of three-momentum transfer, and $Q^2 = q^2 - T^2 > 0$. The response functions

$$\begin{aligned} R_{\mu\nu}^{(w,\gamma)} &= \frac{1}{2J_i + 1} \sum_{M_{J_i}} \sum_f \langle f | j_{w,\gamma}^\mu | i \rangle \sum_f \langle f | j_{w,\gamma}^\nu | i \rangle^* \\ & \quad \times \delta(T + E_i - E_f), \end{aligned} \quad (5)$$

depending on q and T , involve a sum of the final scattering states $|f\rangle$ and a spin average of the initial states $|i\rangle = |J_i, M_{J_i}, \dots\rangle$, and the Dirac delta function imposes energy conservation. The relativistic weak and electromagnetic four-currents are

$$j_w^\mu = \bar{e}' \left[\left(\frac{1}{2} + 2 \sin^2 \theta_W \right) \gamma^\mu - \frac{1}{2} \gamma^\mu \gamma_5 \right] e, \quad (6)$$

$$j_\gamma^\mu = \bar{e}' \gamma^\mu e, \quad (7)$$

where the Greek index $\mu = 0$ and $1, 2, 3$ specify the charge and spatial current densities, respectively, and the direction of \vec{q} is taken to be the quantization axis $\mu = 3$. Note that we perform a Fierz reordering to the weak charged-current interaction (in the four-fermion contact form) and get a more compact cross section formula in Eq. (3), in which j_w^μ is a sum of the charged and neutral currents. Also we apply vector current conservation to relate the longitudinal component j_γ^3 to j_γ^0 , so the response functions $R_{03,30,33}^{(\gamma)}$ are effectively included in Eq. (4).

The many-body theory we adopted in this work to evaluate the germanium response functions is the multiconfiguration relativistic random-phase approximation (MCRRPA) [26, 27]. In essence, this method is based on the time-dependent Hartree-Fock (HF) approximation, however, several important features, as the name suggests, make it a better tool beyond HF to describe transitions of open-shell atoms of high atomic number Z : First, for open-shell atoms, typically there are more

than one configurations which have the desired ground state properties, therefore, a proper HF reference state should be formed by a linear combination of these allowed configurations, i.e., a multiconfiguration reference state. Second, for atoms of high Z , the relativistic corrections can no longer be ignored. By using a Dirac equation, instead of a Schrödinger one, the leading relativistic terms in the atomic Hamiltonian are treated nonperturbatively from the onset. Third, two-body correlation in addition to HF is generally important for excited states and transition matrix elements. The random-phase approximation (RPA) is devised to account for part of the additional two-body correlation (particles can be in the valence or core states) not only for the excited but also for the reference state, and in a lot of cases, it gives good agreement with experiment [28]. Furthermore, it has been shown that RPA equations preserve gauge invariance [29]; this provides a measure of stability of their solutions.

The MCRRPA has been applied successfully to photoexcitation and photoionization of divalent atoms such as Be, Mg, Zn, etc.; some of the results are summarized in [30]. Following similar treatments, we consider the electronic configuration of germanium as a core filled up to the $4s$ orbits, with two valence electrons in the $4p$ orbits. As the Ge ground state is a 3P_0 state, it is a linear combination of two configurations: $[\text{Zn}]4p_{1/2}^2$ and $[\text{Zn}]4p_{3/2}^2$. The wave function is calculated using the multiconfiguration Dirac-Fock (MCDF) package [31]. The atomic excitations due to weak and magnetic scattering are solved by the MCRRPA equation, and consequently transition matrix elements are yielded. In our calculation, all the current operators are expanded by spherical multipoles, and the resulting final scattering states are represented in the spherical wave basis and subject to the incoming-wave boundary condition.

Compared with recent work on the same subject [18, 19] which are also in the similar spirit of relativistic HF, the MCRRPA approach is refined in several respects: (1) As indicated by the near degeneracy of the $N_{II}(4p_{3/2})$ and $N_{III}(4p_{1/2})$ levels in Table I, using a multiconfiguration reference state is necessary. (2) The non-local Fock term is treated exactly, without resorting to the local exchange potentials. (3) The excited states are calculated with two-body correlation built in by MCRRPA, not simply by solving a Coulomb wave function with a static one-hole mean field.

To benchmark our Ge calculation, we first list all the single-particle energies calculated by MCDF and the edge energies extracted from photoabsorption data [25] in Table I. Although they are not fully equivalent, good agreements are seen for the inner shells. The discrepancy in the outer shells mostly comes from the fact that the data are taken from Ge solids whose crystal structure is supposed to modify the atomic wave function. As we shall show later, this is not important for the kinematic range

TABLE I. The single-particle energies of Ge atoms calculated by MCDF (s.p.) versus the edge energies extracted from photoabsorption data (edge) [25] of Ge solids. All energies are in units of eV.

	$K(1s_{\frac{1}{2}})$	$L_I(2s_{\frac{1}{2}})$	$L_{II}(2p_{\frac{1}{2}})$	$L_{III}(2p_{\frac{3}{2}})$	$M_I(3s_{\frac{1}{2}})$	$M_{II}(3p_{\frac{1}{2}})$	$M_{III}(3p_{\frac{3}{2}})$	$M_{IV}(3d_{\frac{3}{2}})$	$M_V(3d_{\frac{5}{2}})$	$N_I(4s_{\frac{1}{2}})$	$N_{II}(4p_{\frac{3}{2}})$	$N_{III}(4p_{\frac{1}{2}})$
s.p.	11185.5	1454.4	1287.9	1255.6	201.5	144.8	140.1	43.8	43.1	15.4	8.0	7.8
edge	11103.1	1414.6	1248.1	1217.0	180.1	124.9	120.8	29.9	29.3			

we are interested. On the other hand, the first ionization energy of the Ge atom in our calculation = 7.856 eV agrees with the experimental value = 7.899 eV [32].

A more definitive test is done with the photoionization process. Unlike the weak and magnetic scattering by neutrinos where the atom absorbs a virtual gauge boson, it is a real photon, with $|\vec{q}| = T$, being absorbed. In Fig. 1, the photoionization cross sections σ_γ for $10 \text{ eV} \leq T \leq 10 \text{ keV}$ from our calculation (for more details, see Ref. [33]) are compared with the fit of experiments [25]. Starting from $T \sim 80 \text{ eV}$, our calculation well reproduces the data curve with an error within 5% in the entire range of T up to 10 keV . For $T < 80 \text{ eV}$, the crystal modification of atomic wave functions becomes important, in particular for the $3d$ orbit as evidenced by the dislocation of its photoionization peak. For later calculations of weak and magnetic scattering, we thus set a minimum of $T_{\min} = 100 \text{ eV}$ —an already ambitious threshold for next-generation detectors—so that the atomic cross section formulae can be applied, and leave the $T < 100 \text{ eV}$ region for future study. On the other hand, an important remark is due here: Photoionization in fact only probes the “on-shell” transverse electromagnetic response functions, i.e., $R_{11+22}^{(\gamma)}|_{q=T}$. One still needs more experiments to completely check the relevant response functions, however, this benchmark test does give one confidence on the applicability of our approach and a realistic error estimate.

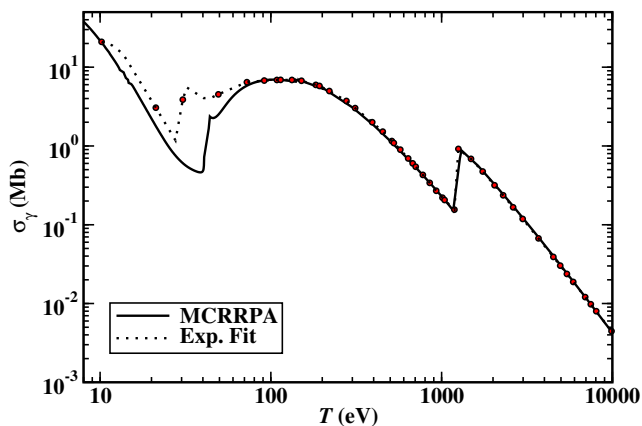


FIG. 1. Germanium photoionization cross section. The solid line is the result of our atomic calculation and the dotted curve is the fit of experimental data (shown in red circles) of Ge solids [25].

Representative results of our full calculations of $\bar{\nu}_e$ -germanium ionization cross sections are shown in Fig. 2; the case with $E_\nu = 1 \text{ MeV}$ is typical for reactor antineutrinos, while $E_\nu = 10 \text{ keV}$ gives an example of low-energy neutrino sources such as tritium β decay (Q value = 18.6 keV), which is considered as one strong candidate to constrain NMMs [34, 35].

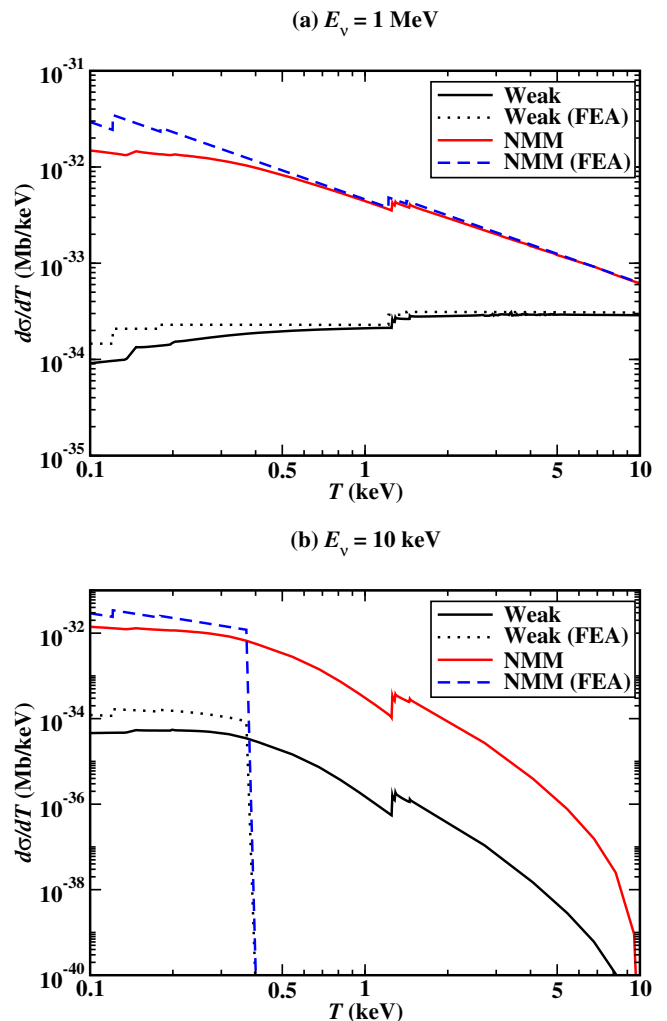


FIG. 2. The differential cross sections of $\bar{\nu}_e$ -germanium ionization with (a) $E_\nu = 1 \text{ MeV}$ and (b) $E_\nu = 10 \text{ keV}$. For magnetic scattering, the neutrino magnetic moment is set to be the current upper limit $\mu_{\bar{\nu}_e} = 2.9 \times 10^{-11} \mu_B$.

As seen from this figure (where $\mu_{\bar{\nu}_e}$ is assumed to be

TABLE II. Limits on NMM at 90% CL with selected reactor neutrino data, comparing cross-sections derived by both MCRRPA and FEA methods. The projected sensitivities are with the parameters shown, together with a benchmark background level of 1/kg-keV-day.

Data	Neutrino Flux ($\text{cm}^{-2}\text{s}^{-1}$)	Data Strength (kg-day)	Threshold (keV)	NMM Limits at 90% CL (μ_B)	
				FEA	MCRRPA
TEXONO 1kg HPG [10]	6.4×10^{12}	ON/OFF : 570.7/127.8	12	$< 7.4 \times 10^{-11}$	$< 7.4 \times 10^{-11}$
TEXONO 900g PPCGe [13]	6.4×10^{12}	ON : 39.5	0.5	$< 1.6 \times 10^{-10}$	$< 1.6 \times 10^{-10}$
TEXONO 500g PPCGe	6.4×10^{12}	ON/OFF : 25.5/13.4	0.3	$< 3.0 \times 10^{-10}$	$< 3.0 \times 10^{-10}$
GEMMA 1.5 kg HPGe [9]	2.7×10^{13}	ON/OFF : 1133.4/280.4	2.8	$< 2.9 \times 10^{-11}$	$< 2.9 \times 10^{-11}$
PPCGe Projected	6.4×10^{12}	(ON/OFF) : 1500/ 500	0.3	$< 2.3 \times 10^{-11}$	$< 2.6 \times 10^{-11}$

the current upper limit $2.9 \times 10^{-11} \mu_B$, the sub-keV measurements with Ge detectors can in principle allow an improved limit by an order of magnitude. On the same plot, we also compare with the results from the free electron approximation (FEA) [17]

$$\frac{d\sigma_{w,\mu}^{(\theta)}}{dT} = \sum_{i=1}^Z \frac{d\sigma_{w,\mu}^{(0)}}{dT} \theta(T - B_i), \quad (8)$$

in which the free electron formulae, Eqs.(1,2), are used for all electrons with binding energies B_i less than T (implemented by the theta function). With both E_ν and T bigger than the relevant atomic scales, it is not a surprise that Eq.(8) gives a good description, as illustrated by Fig.2(a) with $T \gtrsim 1$ keV. However, as T drops down to the sub-keV regime, the atomic binding effect starts to manifest and results in suppression of the differential cross sections, which can be as large as a factor of 0.63 and 0.5 for the weak and magnetic scattering, respectively. On the other hand, for the case of $E_\nu = 10$ keV, the free electron picture fails in the entire range of T , because the minimum de Broglie wavelength that could be reached by the incident neutrino $\lambda \sim 0.1 \text{ keV}^{-1}$ is not much smaller than the mean orbital radius of Ge $\equiv \sum_{i=1}^Z \langle r_i \rangle / Z \sim 0.2 \text{ keV}^{-1}$. Furthermore, the free electron dynamics enforces a cutoff for the maximum of $T_{\text{max}} = 2E_\nu^2 / (2E_\nu + m_e) \approx 0.38 \text{ keV}$ [seen from Fig.2(b)], which differs widely from the physical situation.

To compare with experiments, the spectrum-weighted cross section should be used. It can be derived from the differential cross-sections of Eqs. (3,4), giving

$$\left\langle \frac{d\sigma}{dT} \right\rangle = \frac{\int dE_\nu \phi(E_\nu) \frac{d\sigma}{dT}(E_\nu)}{\int dE_\nu \phi(E_\nu)}, \quad (9)$$

where $\phi(E_\nu)$ is the neutrino spectrum.

Analysis was performed with data taken with standard high-purity germanium (HPGe) and p -type point-contact germanium detectors (PPCGe) with sub-keV sensitivity at the Kuo-Sheng Reactor Neutrino Laboratory (KSNL) [10, 13]. The key experimental parameters and the 90% CL limits are summarized in Table II,

for both MCRRPA and FEA methods. Also listed are the published FEA and derived MCRRPA bounds by the GEMMA experiment [9], and the projected sensitivities for PPCGe under realistic conditions. The TEXONO PPCGe Reactor ON–OFF spectrum with PPCGe from 25.5/13.4 kg-day of ON/OFF data at a threshold of 300 eV and the corresponding NMM squared constraints are displayed in Fig. 3.

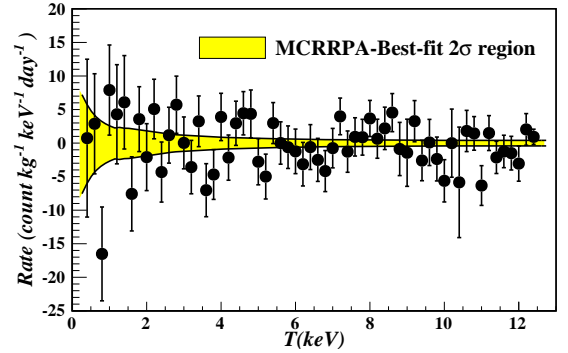


FIG. 3. Reactor ON–OFF residual spectrum with a PPCGe from 25.5/13.4 kg-day of ON/OFF data at KSNL at a threshold of 300 eV. The two-sigma allowed band from MCRRPA analysis is also displayed

In summary, we demonstrate in this work that by using the multiconfiguration relativistic random phase approximation, the atomic structure of germanium and its photoabsorption data with photon energy larger than 100 eV can be reliably calculated. Applying the method to the atomic ionization by the neutrino weak and magnetic moment interactions, it is found that while the conventional scattering formula based on the free electron approximation works reasonably well when the neutrino energy loss is larger than 1 keV, the atomic effect starts to play a significant role for sub-keV energy loss. With new-generation germanium detectors lowering their thresholds down to the sub-keV regime and enhancing their sensitivities to neutrino magnetic moments, our scattering formulae should provide more reliable constraints.

We acknowledge the supports from the National Sci-

ence Council, Republic Of China under Grant Nos. 102-2112-M-002-013-MY3 (JWC, CLW, CPW), 98-2112-M-259-004-MY3 (CPL), and 101-2112-M-259-001 (CPL); the CTS and CASTS of NTU (JWC, CLW, CPW).

-
- [1] H. T. Wong and H. B. Li, *Mod. Phys. Lett. A* **20**, 1103 (2005).
 - [2] C. Broggini, C. Giunti, and A. Studenikin, *Adv. High Energy Phys.* **2012**, 459526 (2012).
 - [3] W. Marciano and A. Sanda, *Phys. Lett. B* **67**, 303 (1977).
 - [4] B. W. Lee and R. E. Shrock, *Phys. Rev. D* **16**, 1444 (1977).
 - [5] K. Fujikawa and R. Shrock, *Phys. Rev. Lett.* **45**, 963 (1980).
 - [6] M. Fukugita and T. Yanagida, *Physics of Neutrinos* (Springer, Berlin, 2003).
 - [7] N. F. Bell, V. Cirigliano, M. J. Ramsey-Musolf, P. Vogel, and M. B. Wise, *Phys. Rev. Lett.* **95**, 151802 (2005); N. F. Bell, M. Gorchtein, M. J. Ramsey-Musolf, P. Vogel, and P. Wang, *Phys. Lett. B* **642**, 377 (2006).
 - [8] P. Vogel and J. Engel, *Phys. Rev. D* **39**, 3378 (1989).
 - [9] A. Beda *et al.*, *Adv. High Energy Phys.* **2012**, 350150 (2012); A. G. Beda *et al.*, *Phys. Part. Nucl. Lett.* **10**, 139 (2013).
 - [10] H. B. Li *et al.*, *Phys. Rev. Lett.* **90**, 131802 (2003); H. T. Wong *et al.*, *Phys. Rev. D* **75**, 012001 (2007).
 - [11] C. Arpesella *et al.*, *Phys. Rev. Lett.* **101**, 091302 (2008).
 - [12] S. T. Lin *et al.*, *Phys. Rev. D* **79**, 061101 (2009).
 - [13] H. B. Li *et al.*, *Phys. Rev. Lett.* **110**, 261301 (2013).
 - [14] W. Zhao *et al.*, *Phys. Rev. D* **88**, 052004 (2013).
 - [15] H. T. Wong, H.-B. Li, and S.-T. Lin, *Phys. Rev. Lett.* **105**, 061801 (2010), erratum: arXiv:1001.2074v3.
 - [16] S. Fayans, V. Y. Dobretsov, and A. Dobrotvetov, *Phys. Lett. B* **291**, 1 (1992).
 - [17] V. I. Kopeikin, L. A. Mikaelyan, V. V. Sinev, and S. A. Fayans, *Phys. At. Nucl.* **60**, 1859 (1997).
 - [18] S. Fayans, L. Mikaelyan, and V. Sinev, *Phys. Atom. Nucl.* **64**, 1475 (2001).
 - [19] V. Kopeikin, L. Mikaelian, and V. Sinev, *Phys. Atom. Nucl.* **66**, 707 (2003).
 - [20] G. Gounaris, E. Paschos, and P. Porfyriadis, *Phys. Lett. B* **525**, 63 (2002).
 - [21] M. B. Voloshin, *Phys. Rev. Lett.* **105**, 201801 (2010), erratum: *ibid.* **106**, 059901 (2011).
 - [22] K. A. Kouzakov and A. I. Studenikin, *Phys. Lett. B* **696**, 252 (2011).
 - [23] K. A. Kouzakov, A. I. Studenikin, and M. B. Voloshin, *Phys. Rev. D* **83**, 113001 (2011).
 - [24] J.-W. Chen, C.-P. Liu, C.-F. Liu, and C.-L. Wu, *Phys. Rev. D* **88**, 033006 (2013).
 - [25] B. L. Henke, E. M. Gullikson, and J. C. Davis, *At. Data Nucl. Data Tables* **54**, 181 (1993).
 - [26] K.-N. Huang and W. R. Johnson, *Phys. Rev. A* **25**, 634 (1982).
 - [27] K.-N. Huang, *Phys. Rev. A* **26**, 734 (1982).
 - [28] M. Y. Amusia and N. A. Chereplov, *Case Stud. At. Phys.* **5**, 47 (1975).
 - [29] D. L. Lin, *Phys. Rev. A* **16**, 600 (1977).
 - [30] K.-N. Huang, H.-C. Chi, and H.-S. Chou, *Chin. J. Phys.* **33**, 565 (1995).
 - [31] J. P. Desclaux, *Comp. Phys. Comm.* **9**, 31 (1975).
 - [32] A. Kramida, Y. Ralchenko, J. Reader, and NIST ASD Team, “NIST Atomic Spectra Database (ver. 5.0),” (2013).
 - [33] J.-W. Chen, H.-C. Chi, C.-P. Liu, C.-L. Wu, and C.-P. Wu, in preparation.
 - [34] Y. Giomataris and J. D. Vergados, *Nucl. Instrum. Meth. A* **530**, 330 (2004).
 - [35] G. C. McLaughlin and C. Volpe, *Phys. Lett. B* **591**, 229 (2004).